Hydrophobically Modified Polyelectrolytes in Dilute Salt-Free Solutions

Andrey V. Dobrynin and Michael Rubinstein*

Department of Chemistry, University of North Carolina,Chapel Hill, North Carolina 27599-3290

Received May 2, 2000; Revised Manuscript Received August 2, 2000

ABSTRACT: The universal diagram of states of hydrophobically modified polyelectrolytes in dilute salt-free solutions is calculated in the framework of the scaling approach. The equilibrium conformations of these polymers were classified using two parameters—geometric and energetic ratios of hydrophobic and polyelectrolyte blocks in unassociated states (the ratio of block sizes and the ratio of block energies). The hydrophobically modified polyelectrolytes self-organize either into necklaces of hairy, crew-cut, or braided micelles or into wormlike cylindrical micelles depending on the values of these two parameters. The universal diagram of states is modified by the counterion condensation.

Introduction

Hydrophobically modified polyelectrolytes are water-soluble polymers that contain small amount of hydrophobic groups.[1,2] These polymers associate in aqueous solutions forming compact conformations similar to those of surfactant or soap micelles and are therefore called "polysoaps". Research during the past four decades (see refs 1 and 2 for review) revealed some general relationships between the molecular architecture and the key properties of polysoaps in aqueous solutions. Polysoaps self-organize into intramolecular micelles in dilute solutions above a certain critical content of hydrophobes. The shapes of these micelles and their numbers per chain are determined by a fine interplay between electrostatic and hydrophobic interactions. In semidilute or concentrated solutions, polysoaps can form intermolecular aggregates. At higher polymer and salt concentrations, the intermolecular associations may be accompanied by a phase separation.

Despite the extensive experimental studies of these polymers, the theoretical understanding of their properties is still incomplete. Theoretical studies of polysoaps are limited to the case of solutions of higher ionic strengths with screened electrostatic interactions. The behavior of polysoap solutions in this regime is similar to the one of neutral amphiphilic macromolecules.[3,4] However, the latest progress in the theory of polyelectrolyte solutions[5−8] provides an opportunity to apply these results to the solutions of polysoaps at various salt and polymer concentrations. In the present paper, we develop a unified scaling theory of thermodynamic properties of charged polysoaps in dilute salt-free solutions.

2. Necklace Structure of Hydrophobically Modified Polyelectrolytes

Consider a hydrophobically modified polyelectrolyte chain consisting of a polyelectrolyte backbone and N_{bl} hydrophobic side blocks with n_A main chain monomers separating neighboring junction points (see Figure 1). The polyelectrolyte backbone therefore contains $N_{bl}n_A$ monomers and each hydrophobic side chain consists of n_B monomers.

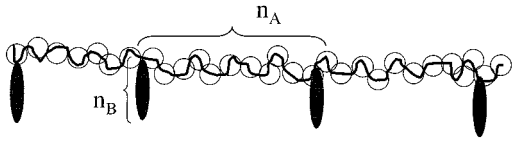

Figure 1. Part of a hydrophobically modified polyelectrolyte (charged polysoap) with the number of polyelectrolyte and hydrophobic blocks N_{bl}, degree of polymerization of polyelectrolyte block n_A, and hydrophobic block n_B.

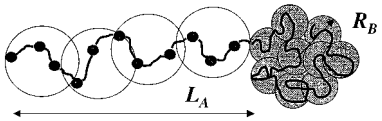

Figure 2. Polyelectrolyte−hydrophobic diblock.

The polyelectrolyte backbone contains a fraction $1/A$ of charged monomers ($n_A/A \gg 1$) and a fraction $(A - 1)/A$ of uncharged monomers. For simplicity, we assume that all monomers have the same size b and the solvent is Θ-like for the monomers of the backbone and is poor for the side chains.

2.1. Polyelectrolyte−Hydrophobic Multiblock. The self-association of a part of a polyelectrolyte−hydrophobic multiblock copolymer into a spherical micelle is controlled by four parameters—the electrostatic energy ϵ_A and the length L_A of a free polyelectrolyte block and the surface energy ϵ_B and the size R_B of an isolated hydrophobic block (globule) (see Figure 2). The equilibrium size of a free polyelectrolyte block is determined by the balance of the two terms of the free energy. The first term is due to the electrostatic repulsion between charged monomers and the second one is the elastic energy of a stand with n_A monomers.

$$F_A \approx \frac{(en_A/A)^2}{\epsilon L_A} + kT\frac{{L_A}^2}{n_A b^2} \qquad (2.1)$$

(Here and below we ignore all numerical prefactors of order unity.) The length of a free polyelectrolyte block is determined by the minimization of the free energy in eq 2.1

$$L_A \approx b n_A {u_A}^{1/3} \qquad (2.2)$$

10.1021/ma000761m CCC: $19.00
Published on Web 09/23/2000

where we have defined a dimensionless interaction parameter

$$u_A = \frac{e^2}{\epsilon kTbA^2} \tag{2.3}$$

The electrostatic energy of this free polyelectrolyte block at its equilibrium length L_A is obtained by substituting eq 2.2 for L_A back into eq 2.1

$$\epsilon_A \approx kTn_A u_A^{2/3} \tag{2.4}$$

The hydrophobic block could either be a $-(CH_2)_{n_B-1}-CH_3$ hydrocarbon tail[9] or a flexible chain of n_B monomers in a poor solvent. In a poor solvent at temperature T below the Θ temperature, the long flexible hydrophobic block forms a globule. The density $\rho \approx b^{-3}\tau$ inside the globule is determined by the balance between the two-body attractive interaction $-kTb^3\tau\rho^2$ (where $\tau = (\Theta - T)/\Theta$ is the reduced temperature) and the three-body repulsive interaction $kTb^6\rho^3$. The size R_B of the globule is

$$R_B \approx (n_B/\rho)^{1/3} \approx b\tau^{-1/3}n_B^{1/3} \tag{2.5}$$

The surface energy of an isolated flexible hydrophobic block in an aqueous solution is

$$\epsilon_B \approx \gamma R_B^2 \approx kTn_B^{2/3}\tau^{4/3} \tag{2.6}$$

where we have defined the surface tension γ of the globule-solvent interface

$$\gamma \approx kT\tau^2/b^2 \tag{2.7}$$

It is useful to define the ratio of the sizes of the two isolated blocks, called the geometric ratio

$$\alpha \approx \frac{R_B}{L_A} \approx \frac{n_B^{1/3}}{\tau^{1/3}u_A^{1/3}n_A} \tag{2.8}$$

and the ratio of their energies

$$\beta \approx \frac{\epsilon_B}{\epsilon_A} \approx \frac{n_B^{2/3}\tau^{4/3}}{n_A u_A^{2/3}} \tag{2.9}$$

called the energetic ratio. Let us consider a micelle formed by aggregation of f polyelectrolyte and f hydrophobic blocks.[10,11] The optimal size of such a micelle is determined by the interplay between the surface energy of the core of the micelle composed of hydrophobic blocks and electrostatic repulsion of polyelectrolyte blocks in the corona. Association of f hydrophobic blocks into one large globule of size

$$R_{core} \approx f^{1/3}R_B \tag{2.10}$$

(the core of the micelle) leads to the surface energy of the core

$$F_{core} \approx \gamma R_{core}^2 \times \epsilon_B f^{2/3} \tag{2.11}$$

This surface energy is lower than that of f individual blocks $\epsilon_B f$. However, this association brings polyelectrolyte blocks together increasing electrostatic energy. The optimal size of the polyelectrolyte corona d_c can be

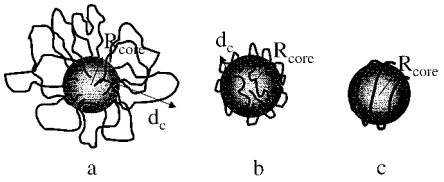

Figure 3. (a) Hairy micelle. (b) Crew-cut micelle. (c) Braided micelle with polyelectrolyte blocks winding around a hydrophobic core.

estimated by minimizing the free energy of the corona

$$F_{corona} \approx kT f^2 n_A^2 u_A \frac{b}{d_c + R_{core}} + kT f \frac{d_c^2}{b^2 n_A} \tag{2.12}$$

The first term is the electrostatic repulsion energy, and the second term is the entropic cost due to stretching of polyelectrolyte blocks. There are three different regimes, as follows.

(i) *Hairy micelles* (Figure 3a)—the size d_c of the corona is larger than the size R_{core} of the core. In this case the size of the micelle d_m is on the order of the size of the corona d_c.

(ii) *Crew-cut micelles* (Figure 3b)—the size of the corona d_c is smaller than the size of the core R_{core} or $d_m \approx R_{core}$.

(iii) *Braided micelles* (Figure 3c)—the electrostatic blocks in the coronas of the crew-cut micelles are self-organized into the spiral braids on the core surface.

The minimization of the free energy (eq 2.12) leads to the optimal size of the corona

$$d_c \approx \begin{cases} L_A f^{1/3}, & \text{for } \alpha < 1 \text{ (hairy micelle)} \\ L_A f^{1/3}\alpha^{-2}, & \text{for } \alpha > 1,\ d_c > L_A \text{(crew-cut micelle)} \end{cases} \tag{2.13}$$

The crossover from the hairy micelle to the crew-cut micelle occurs at $\alpha \approx 1$ or when length of the polyelectrolyte block L_A becomes on the order of the hydrophobic block size R_B. Note that the corona size increases as one-third power of the aggregation number f as if one has a dense packing of polyelectrolyte blocks.[12] The free energy of the corona at equilibrium with a fixed number of blocks per micelle is

$$F_{corona} \approx \begin{cases} \epsilon_A f^{5/3}, & \text{for } \alpha < 1 \\ \epsilon_A f^{5/3}\alpha^{-1}, & \text{for } \alpha > 1 \end{cases} \tag{2.14}$$

The optimal aggregation number is obtained by minimizing the chemical potential of the micelle $\mu = \partial(F_{corona} + F_{core})/\partial f$ that results in the following expressions

$$f \approx \begin{cases} \beta, & \text{for } \alpha < 1 \\ \alpha\beta, & \text{for } \alpha > 1 \end{cases} \tag{2.15}$$

The condition $f > 1$ defines a region in the parametric space where charged polysoaps form micelles. Substituting the equilibrium aggregation number f (eq 2.15) into the expression for the corona size, eq 2.13, one obtains the dependence of the corona size on the parameters of the system

$$d_c \approx \begin{cases} L_A\beta^{1/3}, & \text{for } \alpha < 1 \\ L_A\beta^{1/3}\alpha^{-5/3}, & \text{for } 1 < \alpha^5 < \beta \end{cases} \tag{2.16}$$

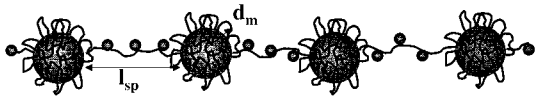

Figure 4. Part of a necklace of spherical flowerlike micelles.

Braided Micelles. At $\beta \approx \alpha^5$ the size of the corona of the crew-cut micelle becomes on the order of the size of the free polyelectrolyte block L_A. For smaller values of the energetic ratio $\beta < \alpha^5$, the electrostatic interactions in the corona of the micelle are dominated by the repulsion between charged monomers on the same polyelectrolyte block, and the size of the polyelectrolyte block saturates at L_A. The polyelectrolyte blocks in the corona of the micelle form a spiral braid[13] winding around the hydrophobic core (see Figure 3c). The winding number n_{spiral} of this spiral braid can be estimated as the ratio of the total length of the polyelectrolyte backbone $fL_A \approx \alpha\beta L_A$ to the core size $f^{1/3}R_B$

$$n_{spiral} \approx \frac{fL_A}{f^{1/3}R_B} \approx \beta^{2/3}\alpha^{-1/3}, \quad \text{for } \sqrt{\alpha} < \beta < \alpha^5 \qquad (2.17)$$

This regime continues while $n_{spiral} > 1$ or for the energetic ratio $\beta > \sqrt{\alpha}$.

Thus, the equilibrium properties of the polyelectrolyte−hydrophobic block copolymer micelles can be characterized by two parameters the geometric ratio α and the energetic ratio β.

2.2. Necklace of Micelles. If hydrophobically modified polyelectrolyte contains a large number $N_{bl} \gg f$ of hydrophobic blocks, it can self-associate into a necklace containing several intramolecular spherical micelles (see Figure 4).

Spacers with Pendant Spherical Globules. The conformation of strings of blocks (spacers) connecting intrachain micelles is determined by the interplay between surface energy of hydrophobic blocks and electrostatic interactions and elastic energy of polyelectrolyte blocks. The spacers separate intrachain micelles reducing the electrostatic repulsion between them. However, they do it at the expense of the hydrophobic energy of nonassociated hydrophobic blocks. These hydrophobic blocks in connecting strings are nonassociated with the surface energy ϵ_B per block. To reduce the number of hydrophobic blocks per spacer the polyelectrolyte blocks stretch until their elastic energy is also on the order of ϵ_B. The length of the spacer block R_A is determined by

$$kT\frac{R_A^2}{b^2 n_A} \approx \epsilon_B \qquad (2.18)$$

The elastic energy of a polyelectrolyte block in the spacer is ϵ_B/ϵ_A times larger than that of a free polyelectrolyte block (eq 2.4). Since a polyelectrolyte block deforms such as a Hookian spring, its size is $\sqrt{\epsilon_B/\epsilon_A} = \sqrt{\beta}$ times larger than the size L_A of a free polyelectrolyte block

$$R_A \approx L_A\beta^{1/2}, \quad \text{for } 1 < \alpha^2 < \beta \qquad (2.19)$$

The size R_A of a spacer polyelectrolyte block is larger than the size R_B of a free hydrophobic block when $\beta > \alpha^2$. If the length of the spacer polyelectrolyte block R_A is longer than the free hydrophobic block R_B, isolated globules along the spacer are far from each other and do not coalesce. The number s of spacer blocks between two neighboring intrachain micelles is determined by the balance of the electrostatic repulsion between micelles and the hydrophobic energy of the spacer blocks

$$\frac{(efn_A/A)^2}{\epsilon s R_A} \approx s\epsilon_B \qquad (2.20)$$

This minimization condition leads to the number of blocks per spacer strand

$$s \approx \begin{cases} \beta^{1/4}, & \text{for } \alpha < 1,\ 1 < \beta \\ \alpha\beta^{1/4}, & \text{for } 1 < \alpha^2 < \beta \end{cases} \qquad (2.21)$$

The mass of a micelle $f(n_A + n_B)$ is much larger than the mass of a spacer $s(n_A + n_B)$ as long as the surface energy ϵ_B of a free hydrophobic block is larger than the electrostatic energy ϵ_A of a free polyelectrolyte block ($\beta > 1$). The length of a string $l_{str} \approx sR_A$ is much longer than the size of a micelle d_m as long as $\beta > \alpha^{4/5}$. Thus, most of the mass of the chain is in micelles, but most of the length is in strings. The total length of the chain in this regime can be estimated as

$$L_{nec} \approx sR_A\frac{N_{bl}}{f} \approx N_{bl}L_A\beta^{-1/4}, \text{ for } 1 < \alpha^2 < \beta \qquad (2.22)$$

It is shorter than the length of a free polyelectrolyte backbone by the factor $\beta^{-1/4}$.

Spacers with Cylindrical Globules. If the length of the spacer polyelectrolyte block R_A becomes shorter than the size of the hydrophobic block R_B the hydrophobic blocks in the strings connecting intrachain micelles aggregate forming a cylinder with the density $\rho \approx \tau b^{-3}$, the length $l_{str} \approx sR_A$ and the width $d_{str} \approx b(n_B b/\tau R_A)^{1/2}$. At equilibrium the surface energy of such hydrophobic cylinder per hydrophobic block is on the order of the elastic energy of the polyelectrolyte block or

$$kT\tau^{3/2}n_B^{1/2}\left(\frac{R_A}{b}\right)^{1/2} \approx kT\frac{R_A^2}{b^2 n_A} \qquad (2.23)$$

The equilibrium length of the spacer block is

$$R_A \approx L_A\alpha^{-1/3}\beta^{2/3} \qquad (2.24)$$

The number s of the blocks in a string connecting intrachain micelles can be found by balancing the electrostatic repulsion between intrachain micelles and elastic energy of the polyelectrolyte blocks

$$\frac{(efn_A/A)^2}{\epsilon s R_A} \approx skT\frac{R_A^2}{b^2 n_A} \qquad (2.25)$$

The number of the blocks in the string is

$$s \approx \alpha^{3/2}, \quad \text{for } 1 < \sqrt{\alpha} < \beta < \alpha^2 \qquad (2.26)$$

The lower boundary for this regime $\beta \approx \sqrt{\alpha}$ is the condition at which (i) the number s of blocks in the string (eq 2.26) becomes on the order of the number of blocks f (eq 2.15) in the intrachain micelle, (ii) the width of the string $d_{str} \approx L_A\alpha^{5/3}\beta^{-1/3}$ becomes on the order of the micelle size $d_m \approx L_A\alpha^{4/3}\beta^{1/3}$, and (iii) the winding

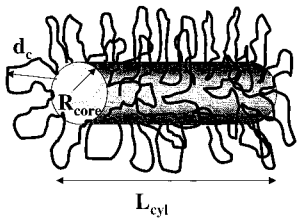

Figure 5. Cylindrical micelle.

number of the spiral braid n_{spiral} (see eq 2.17) becomes on the order of unity. The length of the necklace with cylindrical strings is still controlled by the length of the strings l_{str} connecting the intrachain micelles, and it is given by the following equation:

$$L_{nec} \approx R_A s\frac{N_{bl}}{f} \approx N_{bl}L_A\alpha^{1/6}\beta^{-1/3}, \quad \text{for } 1 < \sqrt{\alpha} < \beta < \alpha^2 \tag{2.27}$$

The total free energy of the hydrophobically modified polyelectrolyte in the necklace configuration is the sum of the free energy of the micelles and of the strings:

$$F_{nec} \approx N_{bl}\epsilon_B\left(\frac{f^{2/3}}{s+f} + \beta^{-1}\frac{N_{bl}L_A}{L_{nec}}\right) \tag{2.28}$$

The average free energy per hydrophobic−polyelectrolyte diblock or the chemical potential of the polyelectrolyte−hydrophobic diblock in the necklace-like aggregate is

$$\mu_{nec} \approx \epsilon_B f^{-1/3} \approx \epsilon_B\begin{cases}\beta^{-1/3}, & \text{for } \alpha < 1, 1 < \beta\\ \beta^{-1/3}\alpha^{-1/3}, & \text{for } 1 < \sqrt{\alpha} < \beta\end{cases} \tag{2.29}$$

At $\beta \approx \sqrt{\alpha}$ the size of the crew-cut micelle becomes on the order of the size of the cylindrical string connecting such micelles and necklace crosses over into a cylindrical aggregate. For smaller values of the energetic ratio $\beta < \sqrt{\alpha}$, the hydrophobically modified polyelectrolyte forms a wormlike (cylindrical) micelle.

3. Cylindrical Micelle

Another possible conformation of a self-associated hydrophobically modified polyelectrolyte is a cylindrical micelle (Figure 5). The cylindrical micelle has a dense core composed of N_{bl} hydrophobic side chains and a corona composed of N_{bl} polyelectrolyte blocks. The collapsed hydrophobic blocks form a cylindrical domain with radius R_{core} and length L_{core}. The polyelectrolyte blocks in the corona of the micelle are extended a typical distance of the corona size d_c. The size of the core can be found by optimizing the sum of the surface energy of the core

$$F_{core} \approx \gamma L_{cyl}R_{core} \approx kT\tau^2\frac{L_{cyl}R_{core}}{b^2} \tag{3.1}$$

and the Coulomb energy of the corona

$$F_{elect} \approx kTu_A{n_A}^2{N_{bl}}^2\frac{b}{L_{cyl}}\ln\left(\frac{L_{cyl}}{d_c + R_{core}}\right) \tag{3.2}$$

at fixed core volume $L_{cyl}{R_{core}}^2 \approx b^3N_{bl}n_B/\tau$ determined by the solvent quality. This minimization leads to the length of micelle

$$L_{cyl} \approx N_{bl}L_A\alpha^{1/3}\beta^{-2/3}, \quad \text{for } 1 < \sqrt{\alpha} < \beta \tag{3.3}$$

and width of the core

$$R_{core} \approx L_A\alpha^{4/3}\beta^{1/3}, \quad \text{for } 1 < \sqrt{\alpha} < \beta \tag{3.4}$$

The length of the hydrophobic core of the cylindrical micelle L_{cyl} becomes on the order of the length of unassociated polyelectrolyte backbone $N_{bl}L_A$ at the value of the energetic ratio β on the order of square root of the geometric ratio α. For smaller values of the parameter $\beta < \sqrt{\alpha}$ the elastic energy of the stretched polyelectrolyte blocks $N_{bl}\epsilon_A$ is larger than the surface energy of the hydrophobic core $N_{bl}\epsilon_B\alpha^{-1/2}$ and controls the length of the cylinder. In this regime the length of the cylindrical aggregate stays the same as that for unmodified polyelectrolyte chain

$$L_{cyl} \approx N_{bl}L_A, \quad \text{for } \beta < \sqrt{\alpha} \tag{3.5}$$

and the thickness of the core is

$$R_{core} \approx L_A\alpha^{3/2}, \quad \text{for } \beta < \sqrt{\alpha} \tag{3.6}$$

The size of the corona d_c can be found by balancing the stretching energy of the polyelectrolyte blocks

$$F_{str} \approx kTN_{bl}\frac{{d_c}^2}{n_A b^2} \tag{3.7}$$

with their electrostatic repulsion F_{elect} (eq 3.2). The equilibrium radius of the corona of the cylindrical micelle of hydrophobically modified polyelectrolyte is

$$d_c \approx \begin{cases}L_A\alpha^{-1/6}\beta^{1/3}, & \text{for } \alpha < 1\\ L_A\alpha^{-5/3}\beta^{1/3}, & \text{for } 1 < \alpha\end{cases} \tag{3.8}$$

The chemical potential of the polyelectrolyte−hydrophobic diblock in the cylindrical micelle is

$$\mu_{cyl} \approx \epsilon_B\begin{cases}\alpha^{-1/3}\beta^{-1/3}, & \text{for } 1 < \sqrt{\alpha} < \beta\\ \beta^{-1}, & \text{for } \beta < \sqrt{\alpha}, \quad \alpha > 1\end{cases} \tag{3.9}$$

4. Diagram of States

Comparison of the chemical potential of a cylindrical micelle (eq 3.9) with that of a necklace-like micelle (eq 2.29) indicates that the necklace conformation of the hydrophobically modified polyelectrolytes has low energy for hairy micelles $\alpha < 1$ and $\beta > 1$. For crew-cut micelles $1 < \sqrt{\alpha} < \beta$ the leading terms of the chemical potential of the hydrophobically modified polyelectrolytes in the necklace and cylindrical conformations are of the same order of magnitude. However, necklace is still a preferred conformation because the length of the necklace L_{nec} in this regimes (see eqs 2.22 and 2.27)) is longer than that of a cylinder L_{core} (eq 3.3) that allows the hydrophobically modified polyelectrolyte to have a lower electrostatic energy because charges are separated by larger distances. This situation is similar to the formation of a necklace in hydrophobic polyelectrolytes.[8,15,17] However, if the opposite inequality holds, $\beta < \sqrt{\alpha}$, the hydrophobically modified polyelectrolytes form cylindrical aggregates. The crossover from a cylindrical aggregate to an unassociated polyelectrolyte chain takes place at $\alpha \approx 1$ when the size of the

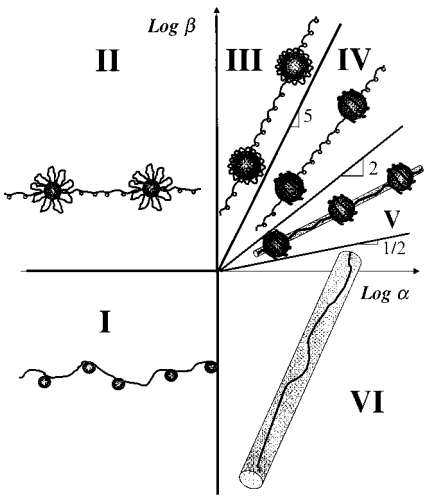

Figure 6. Diagram of state of a hydrophobically modified polyelectrolyte. Regime I corresponds to conformations of polyelectrolyte chains unperturbed by hydrophobic interactions. In regimes II, III, IV, and V, chains form necklaces with the size of the beads controlled by the size of polyelectrolyte corona (II) and by the size of the hydrophobic core (III, IV, V). In regime V, the hydrophobic blocks in the strings of the necklace overlap, forming a cylindrical aggregate. Regime VI corresponds to cylindrical intrachain micelles. Logarithmic scales.

Table 1. Boundaries between Different Regimes for the Diagram of State in Figure 6

I−II	$\beta \approx 1, \alpha \approx 1$
II−III	$\alpha \approx 1, \beta > 1$
III−IV	$\beta \approx \alpha^5, \alpha > 1$
IV−V	$\beta \approx \alpha^2, \alpha > 1$
V−VI	$\beta \approx \sqrt{\alpha}, \alpha > 1$

hydrophobic block in the core of the cylindrical aggregate becomes on the order of the length of the polyelectrolyte block L_A.

In Figure 6 we sketch the diagram of states of hydrophobically modified polyelectrolytes as a function of the geometric ratio α and the energetic ratio β. The boundaries between different regimes are given in Table 1. In region I *(necklace of pendant globules)* ($\alpha < 1, \beta < 1$) the hydrophobic interaction is weaker than electrostatic one and does not lead to intramolecular association. The chain behaves like a polyelectrolyte with pendant hydrophobic globules. In regions II *(necklace of hairy micelles)* ($\alpha < 1, \beta > 1$), III *(necklace of crew-cut micelles)* ($1 < \alpha^5 < \beta$), IV *(necklace of braided micelles)* ($\alpha^2 < \beta < \alpha^5$), and V *(necklace of braided micelles with cylindrical strings)* ($\sqrt{\alpha} < \beta < \alpha^2$), hydrophobically modified polyelectrolyte forms a necklace. The only difference between the conformation of the hydrophobically modified polyelectrolyte in these regimes is that in regime II the size of the intrachain micelles (beads) is controlled by the stretched polyelectrolyte blocks in the coronas of the micelles (hairy intrachain micelles), while in regimes III, IV, and V the size of the coronas is smaller than the size of the cores (crew-cut and braided intrachain micelles). In regimes IV and V, polyelectrolyte blocks in the coronas form spiral braids around the cores. In regimes III and IV, the hydrophobic blocks in the strings form pendant spherical globules. In regime V, they associate into cylindrical globules. In region VI ($1 < \alpha, \beta < \sqrt{\alpha}$), polymer chain forms a wormlike cylindrical micelle.

The predictions of our model can be compared with the previous studies by Turner and Joanny[14] on the self-association of hydrophobically modified polyelectrolytes. These authors considered the self-association of hydrophobically modified polyelectrolytes with soluble backbone and side-chain hydrophobes each of which carries an electric charge at the junction point (the headgroup of a surfactant). They argued that for this particular chemical structure of the hydrophobically modified polyelectrolytes the wormlike (cylindrical) micelles have lower free energy than the necklace-like aggregates. However, their analysis was based on the wrong assumption for the structure of the corona of the micelle. In particular, these authors assumed that the blocks in the corona of the intrachain micelles are equally spaced. This uniform distribution of the corona blocks in beads of the necklace-like aggregates leads to extra stretching making the necklace structure less favorable than the cylindrical one. The spiral braid structure of the polyelectrolyte blocks in the coronas of micelles, proposed in the present paper, lows the free energy of the necklace-like aggregates making it stable thermodynamic structure. The detailed analysis of this model is presented in the Appendix.

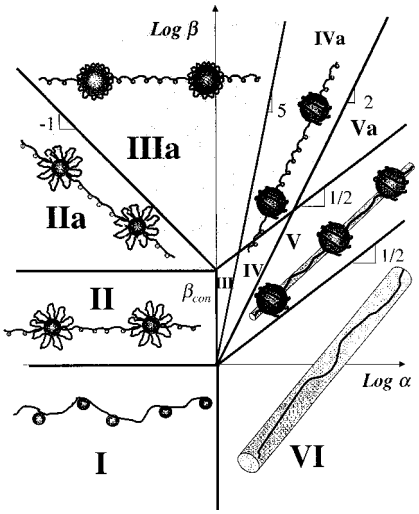

Figure 7. Diagram of state of a hydrophobically modified polyelectrolyte. Shaded area corresponds regimes with counterion condensation. Regime I corresponds to conformations of polyelectrolyte chains unperturbed by hydrophobic interactions. In regimes II, IIa, III, IIIa, IV, IVa, V, and Va, chains form necklaces. Regime VI corresponds to cylindrical micelles. Logarithmic scales.

Table 2. Boundaries between Different Regimes for the Diagram of State in Figure 7

I−II	$\beta \approx 1, \alpha < 1$
II−IIa	$\beta \approx \beta_{con}, \alpha < 1$
IIa−IIIa	$\beta \approx \alpha^{-1}\beta_{con}, \alpha < 1$
IIIa−IVa; III−IV	$\beta \approx \alpha^5, \alpha > 1$
IIIa−III; IV−IVa	$\beta \approx \sqrt{\alpha}\beta_{con}, \alpha > 1$
IV−V; IVa−Va	$\beta \approx \alpha^2, \alpha > 1$
V−Va	$\beta \approx \sqrt{\alpha}\beta_{con}, \alpha > 1$
V−VI	$\beta \approx \sqrt{\alpha}, \alpha > 1$
VI−I	$\alpha \approx 1, \beta < 1$

5. Counterion Condensation

The strong electrostatic attraction between charged groups on the chains and counterions results in the counterion condensation. The crossover conditions between free and condensed counterions can be found by the comparison of the entropic loss due to localization of the counterions and the electrostatic interaction between a counterion and the charges on the chain. We

will consider counterion condensation in different regimes of the diagram of states of hydrophobically modified polyelectrolytes (see Figure 7). The boundaries between different regimes are given in Table 2.

Regime I (Necklace of Pendant Globules) ($\alpha < 1, \beta < 1$). In this regime the polyelectrolyte backbone is stable with respect to counterion condensation as long as the linear charge density on the chain $n_A/(AL_A)$ is smaller than one charge per Bjerrum length $l_B \approx e^2/\epsilon kT$.[18] This condition can be rewritten in terms of the parameters of the system as follows

$$\beta_{con} \approx \frac{bA^{1/2}}{l_B} \gg 1 \tag{5.1}$$

In this range of parameters the electrostatic interaction between two charged monomers separated by A monomers along polymer chain $kTl_B/bA^{1/2}$ is weaker than the thermal energy kT and is not strong enough to perturb the Gaussian conformation of the chain on this length scale.

Regimes II, IIa (Necklace of Hairy Micelles). In the case of the necklace structure the counterion condensation on the beads of the necklace determines the counterion condensation threshold.[8,15,19,20] The intrachain micelles (beads) are stable with respect to counterion condensation as long as the electrostatic interaction between a micelle and a counterion on its surface is smaller than the thermal energy kT

$$\frac{e^2 f n_A}{\epsilon A d_m} < kT \tag{5.2}$$

Combining eqs 2.13 and 2.15, we obtain the stability condition for a micelle with respect to counterion condensation

$$\beta < \beta_{con} \tag{5.3}$$

This stability line ($\beta = \beta_{con}$) is parallel to the transition line ($\beta \approx 1$) between the polyelectrolyte chain regime (I) and the hairy necklace regime (II). Thus, this necklace structure will survive as long as the polyelectrolyte backbone is weakly charged or the parameter $\beta_{con} \gg 1$. Above the counterion condensation threshold, for the energetic ratio β larger than β_{con}, the condensed counterions occupy corona of the micelle and reduce the electrostatic potential of the micelle to the crossover value kT/e fixing the relation between the fraction p_{free} of free counterions, aggregation number of the micelle f, and its size d_m

$$\frac{p_{free} l_B f n_A}{A d_m} \approx 1 \tag{5.4}$$

The fraction of free counterions is small $p_{free} \ll 1$ and most of counterions are trapped inside coronas. The equilibrium size of coronas is now determined by the balance of the osmotic energy of the counterions trapped inside

$$F_{osm} \approx kTf \frac{n_A}{A} \ln\left(f \frac{n_A}{A d_m^3}\right) \tag{5.5}$$

with the elastic energy of the polyelectrolyte blocks

$$F_{elast} \approx kT f \frac{d_c^2}{b^2 n_A} \tag{5.6}$$

This gives the size of the corona of the intrachain micelles

$$d_c \approx b\frac{n_A}{A^{1/2}} \approx L_A \beta_{con}^{1/3} \tag{5.7}$$

To find the equilibrium aggregation number f of the micelle, we have to balance the osmotic energy of counterions inside the corona

$$F_{osm} \approx kTf \frac{n_A}{A} \ln f \tag{5.8}$$

with the surface energy per hydrophobic block in the micellar core $F_{core} \approx \epsilon_B f^{2/3}$. This results in the following dependence of the aggregation number on the parameters of the system.

$$f \approx \left(\frac{\epsilon_B A}{kT n_A}\right)^3 \approx \beta^3 \beta_{con}^{-2} \tag{5.9}$$

The effective charge of an intrachain micelle above the counterion condensation threshold is

$$Q_{eff} \approx \frac{d_m}{l_B} \approx f \frac{n_A}{A}\left(\frac{\beta_{con}}{\beta}\right)^3, \quad \text{regime IIa} \tag{5.10}$$

The length of a string separating two neighboring micelles with the effective charge on each of them Q_{eff} is given by the following equation:

$$l_{str} \approx Q_{eff} R_A \left(\frac{l_B kT}{\epsilon_B R_A}\right)^{1/2} \approx L_A \beta^{-1/4} \beta_{con}, \quad \text{regime IIa} \tag{5.11}$$

The length of the necklace in this regime is

$$L_{nec} \approx \frac{N_{bl}}{f} l_{sp} \approx \frac{L_A N_{bl}}{\beta^{1/4}}\left(\frac{\beta_{con}}{\beta}\right)^3, \quad \text{regime IIa} \tag{5.12}$$

Regimes III, IIIa (Necklace of Crew-Cut Micelles). The crossover from the hairy intrachain micelles regime to the crew-cut intrachain micelle occurs at a corona size comparable with the core size $d_m \approx d_c \approx R_B f^{1/3}$ or at

$$\beta \approx \beta_{con} \alpha^{-1} \tag{5.13}$$

This line separates regimes IIa and IIIa on the diagram of states given in Figure 6. In regime IIIa the aggregation number of the intrachain micelles is still determined by the balance of the osmotic energy of the condensed counterions in the coronas of the micelles with the surface energy of the cores and is given by eq 5.9. The corona of an intrachain micelle has the same size as in regime IIa (see eq 5.7). In this regime the effective charge of the crew-cut micelles is

$$Q_{eff} \approx \frac{R_B f^{1/3}}{l_B} \approx f \frac{n_A}{A} \alpha \left(\frac{\beta_{con}}{\beta}\right)^2, \quad \text{regime IIIa} \tag{5.14}$$

The length of the strings connecting the intrachain micelles with this effective charge is the same as in

regime III

$$l_{str} \approx L_A \alpha \beta^{3/4}, \quad \text{regime IIIa} \tag{5.15}$$

The length of the whole necklace is given by the following equation:

$$L_{nec} \approx \frac{N_{bl}}{f} l_{str} \approx \frac{N_{bl} L_A}{\beta^{1/4}} \alpha \left(\frac{\beta_{con}}{\beta}\right)^2, \quad \text{regime IIIa} \tag{5.16}$$

The boundary between regimes IIIa and III is determined by the counterion condensation condition on the crew-cut micelles

$$\frac{l_B f n_A}{A R_{core}} \approx \frac{u_A A n_A \epsilon_B^{2/3}}{R_B^{1/3} L_A^{2/3} \epsilon_A^{2/3}} \approx 1 \tag{5.17}$$

This condition can be rewritten in terms of the energetic and geometric ratios as follows:

$$\beta \approx \beta_{con} \alpha^{1/2} \tag{5.18}$$

The counterion condensation does not affects the length of the spacer polyelectrolyte block in the strings. The length of this block is still given by eq 2.24.

Regimes IV, IVa (Necklace of Braided Micelles). The counterion condensation condition and necklace parameters for the necklace of braided micelles are similar to the ones discussed above for the case of crew-cut micelles (regimes III and IIIa). Thus, the crossover between regimes IV−V and regimes IVa−Va occurs when the length of the spacer polyelectrolyte block R_A becomes on the order of the size of the hydrophobic block R_B and is at energetic ratio $\beta \approx \sqrt{\alpha}$.

Regimes V, Va (Necklace of Braided Micelles with Cylindrical Strings). The structure of the braided intrachain micelles in regime V is the same as in the regime IV. Therefore, the counterion condensation condition on the intrachain micelles in regime V is given by the same equation (5.18). The equilibrium parameters of the necklace in regime V can be obtained in a way similar to regimes IIa and IIIa (see above). Below, we only quote the final results for the length of the strings connecting the crew-cut micelles

$$l_{str} \approx L_A \alpha^{7/6} \beta^{2/3}, \quad \text{regime Va} \tag{5.19}$$

and for the total length of the necklace

$$L_{nec} \approx \frac{N_{bl} L_A}{\beta^{1/3}} \alpha^{7/6} \left(\frac{\beta_{con}}{\beta}\right)^2, \quad \text{regime Va} \tag{5.20}$$

Regimes VI (Wormlike Micelle). The charged cylindrical aggregate is stable with respect to counterion condensation as long as the linear charge density on the cylindrical aggregate is less than or equal to one per Bjerrum length l_B (for monovalent counterions)[18]

$$\frac{N_{bl} n_A}{A L_{cyl}} \le \frac{1}{l_B} \tag{5.21}$$

Since the length of cylindrical micelle coincides with that of unassociated polyelectrolyte, the counterion condensation condition is the same for both regimes I and VI and is determined by eq 5.1 ($\beta_{con} > 1$).

6. Conclusion

In the present paper, we have considered the equilibrium properties of hydrophobically modified polyelectrolytes in dilute salt-free solutions in the framework of the scaling approach. We have obtained equilibrium conformations of the charged polysoaps in terms of the geometric $\alpha = R_B/L_A$ and energetic $\beta = \epsilon_B/\epsilon_A$ ratios of free hydrophobic and polyelectrolyte blocks. Using these two parameters we were able to construct the universal diagram of states of hydrophobically modified polyelectrolytes (see Figure 6). In a dilute salt-free solution hydrophobically modified polyelectrolyte molecule aggregates into either a necklace of hairy, crew-cut, or braided micelles or into wormlike (cylindrical) micelle. We have also analyzed the effects of counterion condensation on the conformations of charged polysoaps. The results of this study are summarized in Figure 7 that represents the modification of the universal diagram of state (Figure 6) due to condensation of counterions. The counterion condensation results in stabilization of the necklace of the crew-cut micelles in the large portion of the diagram of state, making it the most favorable conformation of the charged polysoaps. The presented classification of the different conformations of charged polysoaps in dilute salt-free solution is the first step toward the understanding the complicated properties of these polymeric systems, and we hope that this paper will inspire experimentalists to test the proposed diagram of states.

Acknowledgment. We are grateful to the donors of the Petroleum Research Fund, administered by the American Chemical Society, for financial support under Grant 34309-AC7 and the National Science Foundation for financial support under Grant DMR-9730777.

7. Appendix

In this appendix, we consider the self-association of hydrophobically modified polyelectrolytes with soluble backbones and side-chain hydrophobes each of which is carrying an electric charge at the junction point—the headgroup of a surfactant (see schematic picture of a chain in the regime I of the Figure 8). For this model our parameter A—the number of neutral monomers between charges—is equal to n_A—the degree of polymerization of the polyelectrolyte block. In this case the average distance L_A per polyelectrolyte block can be obtained by substituting $n_A = A$ into eqs 2.2 and 2.4

$$L_A \approx b u^{1/3} A^{1/3} \tag{7.1}$$

and the average electrostatic energy per block is

$$\epsilon_A \approx kT u^{2/3} A^{-1/3} \tag{7.2}$$

in the unassociated state. In the last two equations, we have introduced the dimensionless parameter $u = l_B/b$. The energy ϵ_B and the size R_B of the hydrophobic block in the unassociated state are the same as in our original

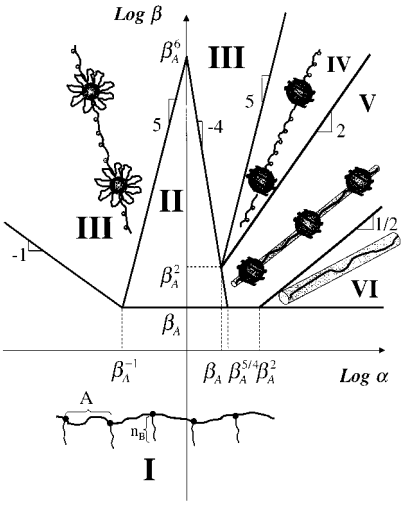

Figure 8. Diagram of state of a hydrophobically modified polyelectrolyte with charges at the junctions between hydrophobic side chains and backbone. Regime I corresponds to conformations of polyelectrolyte chains unperturbed by hydrophobic interactions. In regime II the formation of the intrachain micelle is controlled by the excluded volume interactions. In regimes III, IV, and V, chains form necklaces of micelles. In regime V, the hydrophobic blocks in the strings of the necklace overlap forming a cylindrical aggregate. Regime VI corresponds to cylindrical intrachain micelles. Logarithmic scales.

model (see section 2). Thus, we can define the energetic ratio

$$\beta \approx \left(\frac{n_B^2 \tau^4 A}{u^2}\right)^{1/3} \tag{7.3}$$

and geometric ratio

$$\alpha \approx \left(\frac{n_B}{\tau u A}\right)^{1/3} \tag{7.4}$$

for the Turner and Joanny polysoaps.[14]

Intrachain Micelles Stabilized by the Excluded Volume Interactions. Consider the formation of the intrachain micelles stabilized by the excluded volume interactions. The optimal size of such micelles is determined by the interplay between the surface energy of the core of the micelle composed of hydrophobic blocks and excluded volume interactions between monomers in the micellar corona. Association of f hydrophobic blocks into one large globule of size given by eq 2.10 (the core of the micelle) leads to the surface energy of the core (see eq 2.11)

$$F_{core} \approx \gamma R_{core}^2 \approx \epsilon_B f^{2/3} \tag{7.5}$$

The contribution of the excluded volume interactions in the corona of the hairy micelle can be estimated from the Daoud−Cotton model of a star[21,22]

$$F_{corona} \approx kT f^{3/2} en\left(\frac{d_{corona} + R_{core}}{R_{core}}\right) \tag{7.6}$$

where the corona size of the hairy micelles is equal to[22,23]

$$d_{corona} \approx b f^{1/4} A^{1/2} \tag{7.7}$$

By minimizing the chemical potential of the micelle with respect to the aggregation number f, one obtains

$$f \approx \left(\frac{\epsilon_B}{kT}\right)^{6/5} \approx (\beta/\beta_A)^{6/5}, \quad \text{hairy micelle} \tag{7.8}$$

where we have defined

$$\beta_A \approx kT/\epsilon_A \approx A^{1/3} u^{-2/3} \tag{7.9}$$

The condition $f > 1$ ($\beta > \beta_A$) defines the region in the parameter space where the hydrophobically modified polyelectrolyte forms intrachain micelles stabilized by the excluded volume interactions. Substituting the equilibrium aggregation number f (eq 7.8) into the expression for the core size (eq 2.10) and corona size (eq 7.7), one obtains the core size

$$R_{core} \approx R_B(\beta/\beta_A)^{2/5}, \quad \text{hairy micelle} \tag{7.10}$$

and the corona size

$$d_{corona} \approx L_A \beta_A^{1/5} \beta^{3/10}, \quad \text{hairy micelle} \tag{7.11}$$

in terms of the energetic ratio β. The crossover from the hairy micelles to the crew-cut micelles occurs when the size of the core R_{core} becomes on the order of the size of the corona d_{corona}. This takes place along the line

$$\beta \approx \beta_A^6 \alpha^{-10} \tag{7.12}$$

Thus, for the range of the energetic ratios $\beta_A < \beta < \beta_A^6\alpha^{-10}$, the hydrophobically modified polyelectrolytes associate into hairy micelles stabilized by the excluded volume interactions.

For the crew-cut micelles ($\beta_A < \beta$; $\beta_A^6\alpha^{-10} < \beta$), the structure of the corona is similar to that of the planar brush with the average distance between grafted chains $d \approx R_{core} f^{-1/2}$ (see ref 23 for review). The excluded volume interactions per polymer strand in the planar brush can be estimated as the thermal energy kT times the number of blobs A/g_d of size d ($g_d b^2 \approx d^2 \approx R_{core}^2/f$). The total free energy of the corona of the crew-cut micelle is equal to the energy per strand $kT\, Afb^2/R_{core}^2$ times the aggregation number f of the micelle

$$F_{corona} \approx kT f^2 \frac{Ab^2}{R_{core}^2} \approx kT f^{4/3} \alpha^{-2} \beta_A \tag{7.13}$$

Balancing this free energy of the corona with the surface energy of the core (eq 7.5), one obtains the equilibrium aggregation number f of the crew-cut micelle.

$$f \approx \alpha^3 \beta^{3/2} \beta_A^{-3}, \quad \text{crew-cut micelle} \tag{7.14}$$

The core size of the micelles with this aggregation number is

$$R_{core} \approx R_B \alpha \beta^{1/2}/\beta_A, \quad \text{crew-cut micelle} \tag{7.15}$$

Electrostatically Stabilized Intrachain Micelles. The analysis presented above is only correct when the excluded volume interactions in the corona of the micelle are stronger than the electrostatic interactions. The electrostatic interactions between charged monomers in the corona of micelle

$$\frac{F_{el}}{kT} \approx \frac{l_B f^2}{R_{core}} \approx \frac{l_B}{R_B} f^{5/3} \approx \begin{cases} \frac{\epsilon_A}{\alpha}\left(\frac{\beta}{\beta_A}\right)^2, & \text{hairy micelle} \\ \frac{\epsilon_A}{\alpha}\left(\frac{\alpha\beta^{1/2}}{\beta_A}\right)^5, & \text{crew-cut micelle} \end{cases} \quad (7.16)$$

start to dominate over the excluded volume ones (eqs 7.6 and 7.13) at values of the energetic ratio β larger than $\beta_A{}^6\alpha^5$ for hairy micelles and $\beta_A{}^6\alpha^{-4}$ for crew-cut micelles. Thus, the lines

$$\beta \approx \begin{cases} \beta_A{}^6\alpha^5, & \text{hairy micelle} \\ \beta_A{}^6\alpha^{-4}, & \text{crew-cut micelle} \end{cases} \quad (7.17)$$

define the boundary in the $\alpha-\beta$ plane between electrostatically dominated and excluded-volume dominated regimes (see Figure 8).

For electrostatically stabilized micelles the equilibrium aggregation number is determined by balancing the surface energy of the core of the micelle (eq 7.5) with the electrostatic repulsion between charged monomers in the corona $l_B f^{5/3}/R_B$. The equilibrium aggregation number for such a micelle is

$$f \approx \alpha\beta \quad (7.18)$$

The self-association of the hydrophobic blocks into electrostatically stabilized intrachain micelles takes place at $f > 1$ or for the values of energetic ratio

$$\beta > \alpha^{-1} \quad (7.19)$$

(see Figure 8).

The charged monomers are uniformly distributed along the surface of the micellar core as long as the average distance between them $R_{core}/\sqrt{f} \approx R_B/(\alpha\beta)^{1/6}$ is smaller than the Gaussian size $b\sqrt{A}$ of the strand with A monomers. This condition can be rewritten in terms of the energetic and the geometric ratios as follows $\beta \approx \beta_A{}^{-3}\alpha^5$. For smaller values of the energetic ratio

$$\beta < \beta_A{}^{-3}\alpha^5 \quad (7.20)$$

the charges on the surface of the micelle form a spiral braid of electrostatic blobs with size $D_e \approx b(A^2/u)^{1/3}$ and number of monomers $g_e \approx (A^2/u)^{2/3}$ in them[5,6,24] winding around the hydrophobic core (see Figure 3c). The winding number n_{spiral} of the spiral braid can be estimated as the ratio of the total length of the polyelectrolyte backbone fAD_e/g_e to the core size $f^{1/3}R_B$

$$n_{spiral} \approx \frac{fAD_e}{g_e f^{1/3} R_B} \approx \beta^{2/3}\alpha^{-1/3} \quad (7.21)$$

The conditions for the aggregation of electrostatically stabilized charged polysoaps into different intrachain aggregates as well as their equilibrium parameters can be derived in a way similar to that discussed in sections 2, 3, and 4. This analysis shows that the hydrophobically modified polyelectrolyte molecules can self-associate into necklaces of micelles with hydrophobic blocks in the strings forming pendant spherical globules or coalesce into cylindrical globules and into wormlike (cylindrical) micelles.

The diagram of states for this model is shown in Figure 8. The association of the hydrophobic side chains into micelles is possible above the line $\beta \approx \beta_A \approx kT/\epsilon_A$. In region I ($\beta < \beta_A, \beta < \alpha^{-1}$) the hydrophobic interactions are weaker than electrostatic and excluded volume ones and do not lead to intramolecular association. The chain behaves like a polyelectrolyte with hydrophobic side chains. In regions II ($\beta_A < \beta < \beta_A{}^6\alpha^5$, $\beta_A < \beta < \beta_A{}^6\alpha^{-4}$) the formation of the intrachain micelles is controlled by excluded volume interactions (see for review, ref 4). The detailed analysis of the excluded volume effects on the association of hydrophobically modified polyelectrolyte molecules is beyond the scope of this paper and will be considered in a separate publication. In regimes III ($\alpha^{-1} < \beta$, $\beta_A{}^{-3}\alpha^5 < \beta$, $\beta_A{}^6\alpha^5 < \beta$, $\beta_A{}^6\alpha^{-4} < \beta$), IV ($\beta_A{}^6\alpha^{-4} < \beta$, $\alpha^2 < \beta < \beta_A{}^{-3}\alpha^5$ for $\alpha > 1$), and V ($\sqrt{\alpha} < \beta < \alpha^2$, $\beta_A < \beta$) a hydrophobically modified polyelectrolyte chain forms a necklace. In regimes IV and V polyelectrolyte blocks in the coronas of micelles form spiral braids around the cores. In regime III and IV the hydrophobic blocks in the strings form pendant spherical globules. In regime V they associated into cylindrical globules. In region VI ($\beta_A < \beta < \sqrt{\alpha}$) polymer chain forms a wormlike cylindrical micelle.

References and Notes

(1) Morishima, Y. Unimolecular Micelles of Hydrophobically Modified Polyelectrolytes. In *Solvents and Self-organization of Polymers*; Weber, S. E., et al., Eds.; p 331.
(2) Laschevskii, A. Molecular Concepts, Self-Organization and Properties of Polysoaps. Adv. Polym. Sci. **19XX**, *124*, 3−88.
(3) Borisov, O. V.; Halperin, A. *Langmuir* **1995**, *11*, 2911.
(4) Borisov, O. V.; Halperin, A. *Curr. Opin. Colloid Interface Sci.* **1998**, *3*, 415.
(5) DeGennes, P.-G.; Pincus, P.; Velasco, R.; Brochard, F. *J. Phys. (Paris)* **1976**, *37*, 1461.
(6) Dobrynin, A. V.; Rubinstein, M.; Colby, R. H. *Macromolecules* **1995**, 28, 1859.
(7) Barrat, J.-L.; Joanny, J.-F. Polyelectrolyte Solutions. In *Advances in Chemical Physics*; Prigogine, I., Rice, S. A., Eds.; John Wiley and Sons: New York, 1996; Vol XCIV, pp 1−140.
(8) Dobrynin, A. V.; Rubinstein, M. *Macromolecules* **1999**, 32, 915−922.
(9) For example, for alkyl side chains, the volume v_0 occupied by a chain of n-hydrocarbons in the core of the micelle is $v_0 \approx (0.027 + 0.027(n_B - 1))$ nm^3 The surface energy of the hydrocarbon/water interface $\gamma \approx 45$ mN/m, and the free energy gain due to transfer of the hydrocarbon tail into the core of the micelle is $\epsilon_B \approx kT(2.55 + 1.25(n_B - 1))$.
(10) Marko, J. F.; Rabin, Y. *Macromolecules* 1992, 25, 1503.
(11) Shusharina, N. P.; Nyrkova, I. A.; Khokhlov, A. R. *Macromolecules* **1996**, 29, 3167.
(12) Borisov, O. V. *J. Phys II* **1996**, *6*, 1.
(13) The helical structure of the polyelectrolyte corona has a lower energy $F_{helix} \approx kTfL_A{}^2/b^2n_A \approx \epsilon_A\alpha\beta$ than that of the corona formed by the equally spaced polyelectrolyte blocks with the distance along the surface of the micelle between two neighboring grafting points $d_{||} \approx f^{-1/2}R_{core}$ (see Turner and Joanny[14]). $F_{stret} \approx kTfd_{||}{}^2/b^2n_A \approx \epsilon_A\beta^{2/3}\alpha^{8/3}$, for $\sqrt{\alpha} < \beta < \alpha^5$.
(14) Turner, M. S.; Joanny, J. F. *J. Phys. Chem.* **1993**, *97*, 4825.
(15) Dobrynin, A. V.; Rubinstein, M. R.; Obukhov, S. P. *Macromolecules* **1996**, 29, 2974.
(16) Micka, U.; Holm, C.; Kremer, K. *Langmuir* **1999**, 15, 4033.
(17) Lyulin, A.; Dunweg, B.; Borisov, O. V.; Dariinski, A. *Macromolecules* **1999**, 32.
(18) Manning, G. S. *J. Chem. Phys.***1969**, *51*, 924.
(19) Schiessel, H.; Pincus, P. *Macromolecules* **1998**, 31, 7953.
(20) Schiessel, H. *Macromolecules* **1999**, 32, 5673.
(21) Daoud, M.; Cotton, J.-P *J. Phys. (Paris)* 1982, 43, 531.
(22) Birshtein, T. M.; Zhulina, E. B. *Polymer* **1984**, 25, 1453.
(23) Halperin, A.; Tirrel, M.; Lodge, T. *Adv. Polym. Sci.* **1991**, 100.
(24) At the length scales on the order of electrostatic blob size $D_e \approx bg_e{}^{1/2}$, the electrostatic interactions between charged monomers $kTl_Bg_e{}^2/A^2D_e$ become on the order of the thermal energy kT.

MA000761M